Microsc. Microanal. 16, 132–136, 2010
doi:10.1017/S1431927610000097

Microscopy AND Microanalysis

Imaging Resin-Cast Osteocyte Lacuno-Canalicular System at Bone-Bioactive Glass Interface by Scanning Electron Microscopy

Alejandro A. Gorustovich

Research Laboratory, National Atomic Energy Commission (CNEA-Reg. Noroeste) and National Research Council (CONICET), Salta, A4408FTV, Argentina

Abstract: The morphology of the osteocyte lacuno-canalicular system at the bone-biomaterial implant-interface has not been fully investigated. In this study, the resin-cast scanning electron microscopy technique was used, for the first time, to image the lacuno-canalicular network within neoformed bone around bioactive glass (BG) particles implanted in rat tibia bone marrow. The most salient finding was that the osteocyte canaliculi pass through the calcium-phosphorus layer formed at the bone-BG interface and reach the silica-rich layer of the reacted BG.

Key words: resin-cast SEM, osteocytes, lacuno-canalicular system, bioactive glass

Introduction

Osteocytes are nonproliferative, terminally differentiated cells of osteoblast lineage comprising 90–95% of all bone cells (Bonewald, 2008; Noble, 2008). They reside, locked inside small lacuna spaces, both in the mineralized bone matrix and in newly formed osteoid (osteoid-osteocytes) (Franz-Odendaal et al., 2006; Noble, 2008). Osteocytes form an extensive connecting syncitial network via cytoplasmic/dendritic processes that pass through the bone in thin canals called canaliculi connecting osteocytes with each other and with cells on the bone surface (Knothe-Tate et al., 2004; Bonewald, 2008). Osteocytes are thought to sense mechanical strain and coordinate adaptive bone-remodeling responses (Aarden et al., 1994; Bonewald, 2008; Bonewald & Johnson, 2008). In addition, it has been proposed that these cells may regulate phosphorus homeostasis, and that the osteocyte lacuno-canalicular network in bone may function as an endocrine organ (Feng et al., 2006; Fukumoto & Martin, 2009; Teti & Zallone, 2009).

The morphology of the lacuno-canalicular system at the bone-biomaterial implant-interface has not been fully investigated. Bioactive glasses (BGs) have been the subject of intensive research in view of their stimulatory effect on bone tissue formation. The osteogenic response to BGs has been widely demonstrated in both *in vitro* and *in vivo* studies. The bioactivity of these silicate and phosphate systems has been attributed to both surface reactions taking place at the material-tissue interface and to the direct effect of glass dissolution products on osteogenesis (Hench et al., 2004; Bosetti & Cannas, 2005; Radin et al., 2005). Bosetti and Cannas (2005) showed that BG particles create a template for osteoblast differentiation of bone marrow stromal cells and mineralized tissue formation *in vitro*. In addition, Radin et al. (2005) demonstrated that biomimetically modified BG increases the rate at which multipotential rat bone marrow stromal cells will undergo osteogenesis. It has also been demonstrated that BG particles are osteoconductive when implanted inside the intramedullary canal of rat tibiae. Histological analysis using undecalcified sections showed that new lamellar bone had formed along the surface of BG particles within four weeks (Gorustovich et al., 2002, 2006, 2007, 2010). However, the morphology of the lacuno-canalicular system at the bone-BG implant-interface has not been investigated to date. The resin-casted scanning electron microscopy (SEM) method, which has been used previously for imaging dentin (Martin et al., 1978; Weber, 1983; Lu et al., 2007), gives a three-dimensional (3D) view of the osteocyte lacuno-canalicular system, by two-dimensional SEM (Weber, 1983; Curtis et al., 1985; Okada et al., 2002; Feng et al., 2006). In this technique, a polished surface from a resin embedded bone is etched with acid to remove mineral, leaving a relief cast of the nonmineralized areas that have been infiltrated by resin, including the osteocyte lacuno-canalicular system, osteoid, and bone marrow. Thus, the aim of the present study was to use the resin-cast SEM technique to image the osteocyte lacuno-canalicular network within neoformed bone around BG particles implanted in rat tibia bone marrow.

Received September 17, 2009; accepted January 13, 2010
E-mail: agorustovich@gmail.com

Materials and Methods

Animals

Male Wistar rats (n:5) (International Laboratory Code Registry: Hsd:Wi-ffyb) weighing 100 ± 20 g were used throughout. The animals were not given a special diet. They were fed rat chow and given water *ad libitum*, housed in steel cages and maintained on a 12:12 h light/dark cycle. The guidelines of the National Institutes of Health (NIH) for the care and use of laboratory animals (NIH Publication No. 85-23, Rev. 1985) were observed.

Bioactive Glass

Strontium-doped glass (45S5.6Sr) was prepared using 6 wt% SrO as a substitute for the CaO in 45S5 BG of nominal composition (45% SiO_2, 24.5% CaO, 24.5% Na_2O, and 6% P_2O_5 in wt%). After the melting process, the glass was cast into a graphite mold, crushed, and sieved to 300–350 μm particles, as described elsewhere (Gorustovich et al., 2010).

Surgical Procedure

All the animals were anesthetized by intraperitoneal administration of a 4:1 solution of ketamine/xylazine, i.e., ketamine chlorhydrate, 50 mg/mL (Ketamina 50® Holliday-Scott, Buenos Aires, Argentina) and xylazine, 20 mg/mL (Rompun® Bayer, Buenos Aires, Argentina) at a dose of 0.15 mL per 100 g body weight. The skin was disinfected and shaved. A longitudinal 1.5 cm incision was made along the frontal aspect of both tibiae. The subcutaneous tissue, muscles, and ligaments were dissected to expose the external surface of the tibiae in the area of the diaphyseal bone. An end-cutting bur (1.5 mm in diameter) was used to drill a hole reaching the bone marrow. Overheating and additional bone damage were prevented by using manual rotating impulsion.

45S5.6Sr BG particles (15 mg) were placed inside the medullary compartment of the tibiae. The wounds were carefully sutured with an absorbable polyglactin 910 suture (Vicryl, Ethicon Inc., New Jersey). The animals were sacrificed 30 days after implantation by an intraperitoneally administered overdose of sodium pentobarbital. The tibiae were resected, fixed in 20% formalin solution, and cleaned of soft tissue.

Resin Embedding and Acid-Etching

The undecalcified tibiae were processed for embedding in methyl-methacrylate (MMA) resin. The samples were then sectioned manually with a saw (Eclipse 32 TPI, Spear & Jackson, England) to obtain 500 μm slices, perpendicular to the major axis of the tibiae, that is, in the middle of the implant bed and two points equidistant from the middle. The cross sections were ground using a grinding machine (Silmar Productos Ópticos-Argentina) and finished manually with sandpaper to obtain sections about 50 μm thick. For resin-casted osteocyte lacuno-canalicular SEM, the samples were conditioned in keeping with the technique described by Feng et al. (2006). Briefly, the surface of ground sections was acid etched with 37% phosphoric acid for 10 s, washed in distilled water for 2 min five times, immersed in 5% sodium hypochlorite for 5 min, washed in distilled water for 2 min five times, air-dried overnight, and then coated with gold and palladium and examined in a scanning electron microscope (JEOL JSM 6480 LV, Japan). In addition, several specimens were carbon-coated in a vacuum evaporator (CAR 001-0045) for Energy Dispersive X-ray (EDX) analysis (Thermo Electron, NORAM System SIX NSS-100). The silicon (Si Kα), calcium (Ca Kα), and phosphorus (P Kα) elements were mainly analyzed at the bone-BG interface at a voltage of 15 kV. The Ca/P ratio was determined.

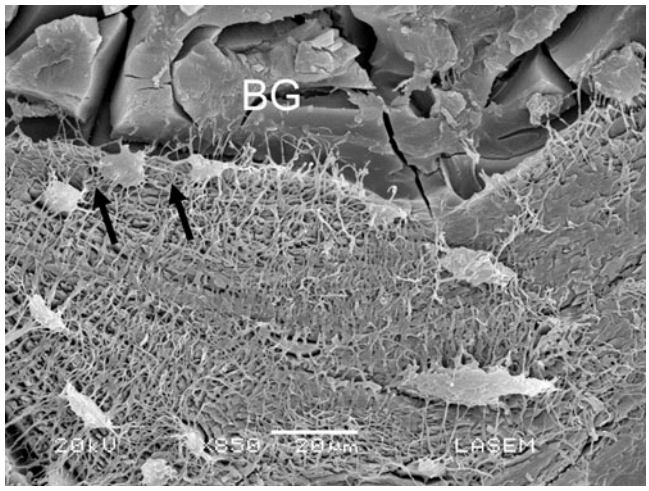

Figure 1. SEM image of acid-etched resin-embedded neoformed bone around a BG particle. Note the numerous osteocyte canaliculi (arrows) that interconnect lacunae.

Results and Discussion

This is the first study to use the resin-cast SEM technique to image and characterize ground sections of undecalcified rat bone tissue with *in situ* bioceramic implants. It has been shown that by etching first the mineral and then the organic component of the bone surrounding MMA-filled osteocyte canaliculi and lacunae, a replica of the morphology of the lacuno-canalicular system at the bone-BG interface can be produced. SEM images showed numerous canaliculi with smooth inner surfaces and extensive branching (Fig. 1). The canaliculi were generally straight and ran perpendicular to the long axis of the osteocyte lacunae. The most salient finding of the present study was that the canaliculi pass through the calcium-phosphorus layer formed at the

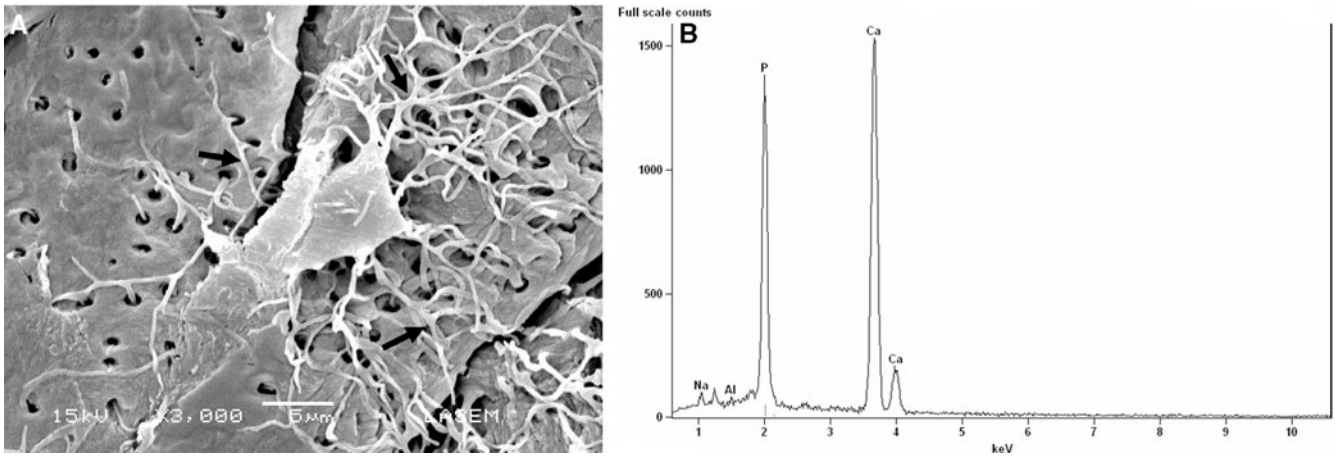

Figure 2. A: An SEM micrograph of a resin cast of a representative osteocyte lacuna with extensive canalicular branching (arrows) at the bone-BG interface. Note that the canaliculi pass through the calcium-phosphorus layer. **B:** EDX spectra of the calcium-phosphorus layer formed at the bone-BG interface.

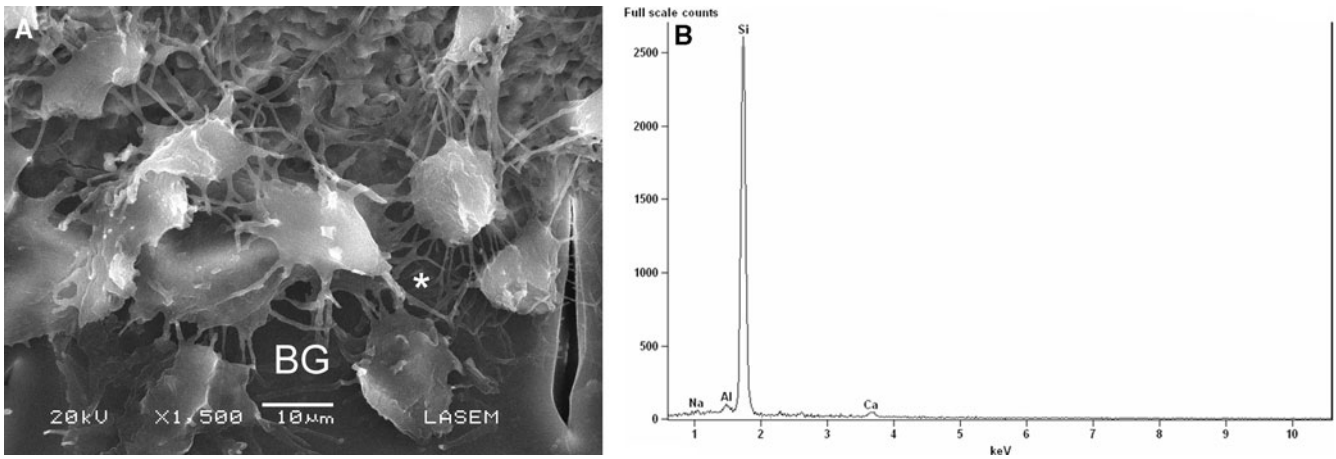

Figure 3. A: SEM image of the acid-etched, resin-casted osteocyte-canalicular system of bone around a BG particle. The white asterisk indicates a region with osteocyte dendritic processes intimately associated with the BG surface. **B:** EDX spectra of the silica-rich layer of the reacted BG.

bone-BG interface (Fig. 2A,B) and reach the silica-rich layer of the reacted BG (Fig. 3A,B).

The key feature that leads to the bone-bonding ability of surface bioactive ceramics (i.e., BGs) is the formation of crystalline hydroxyapatite (HA) on their surface (Hench, 1991; Kokubo & Takadama, 2006; Lee et al., 2006). Following contact with a physiological fluid, the deposition of HA on the surface of silicate BGs containing calcium, phosphorous, and alkali metals occurs through a sequence of consecutive stages as described by Hench (1991): (1) Na^+ ions are rapidly released and replaced by H^+ from the solution, (2) the corresponding increase in local pH promotes breaking of surface Si-O-Si bonds and release of soluble silica to the solution, (3) some of the surface silanol groups formed in steps (1) and (2) condense to form a hydrated silica-rich layer on the surface, (4) calcium (Ca) and phosphate (P) ions are released through the surface silica layer and incorporate other Ca and P ions from solution to form an amorphous calcium phosphate phase deposited on the surface, and (5) the latter amorphous film incorporates additional carbonate ions from solution and crystallizes to HA. In the present study the Ca/P ratio (1.78 ± 0.02) obtained by EDX microanalysis for the calcium-phosphorus layer formed at the bone-BG interface was in the range of the values expected for apatites.

It has been described that the early formation of dendrites by embedding osteoid-osteocytes is polarized toward the mineralization front to which cellular processes are

oriented (Palumbo et al., 2004; Bonewald, 2005). The present study provides evidence that osteocyte dendritic processes could become entrapped in the mineralized phase deposited on the surface of BG particles. Dendrites may be essential for osteocyte function, viability, and response to load (Bonewald, 2005). Within this context, future studies will be devoted to clarify the functional relevance of the results afforded by the present experimental model.

In addition to the resin-cast SEM technique, there are alternative methods to study the osteocyte lacuno-canalicular system. It has been reported that it was possible to observe the osteocyte network by labeling the cells with fluorochromes (i.e., Procion red, fluorescently labeled phalloidin) and using confocal laser scanning microscopy (CLSM) (Knothe-Tate et al., 1998; Kamioka et al., 2001; Sugawara et al., 2005; Feng et al., 2006; Xie et al., 2008). Moreover, several approaches are being explored to provide quali-quantitative information respecting the 3D osteocyte lacunar system at high spatial resolution. These include the use of atomic force microscopy (Reilly et al., 2001), synchrotron radiation (SR)-based nanocomputed tomography (nano-CT) (Schneider et al., 2007) and, more recently, ultrahigh voltage electron microscope tomography (Kamioka et al., 2009). In this regard, the success of the SR nano-CT to assess quantitatively the ultrastructural bone properties is based on the broader application of this method to investigate the osteocyte lacuno-canalicular system at the bone-biomaterial interface in 3D in a fully nondestructive fashion. This advantage is not accessible with all the other techniques mentioned above. However, it should be noted that with SR, the specimen sizes are relatively small, and the equipment is available only at centralized facilities. In contrast, the resin-cast SEM technique is relatively inexpensive and therefore more widely available. Sample preparation is simple, and the rapid data acquisition time and the absence of facility time restrictions expedite analysis of multiple samples. However, SEM does not allow volume analysis, and slice preparation can modify the structure of the bone-biomaterial interface.

Conclusion

The resin-cast SEM technique provided here represents a simple methodology that allows for easy visualization of the osteocyte lacuno-canalicular system at the bone-BG interface.

Acknowledgments

The author gratefully acknowledges the expert assistance of Pedro Villagrán, Ch.E., and Silvia Blanco, Ch.E. with SEM-EDX, LASEM–ANPCyT-UNSa-CONICET, Salta, Argentina.

References

Aarden, E.M., Burger, E.H. & Nijweide, P.J. (1994). Function of osteocytes in bone. *J Cell Biochem* **55**, 287–299.

Bonewald, L.F. (2005). Generation and function of osteocyte dendritic processes. *J Musculoskelet Neuronal Interact* **5**, 321–324.

Bonewald, L.F. (2008). Osteocytes. In *Primer on the Metabolic Bone Diseases and Disorders of Mineral Metabolism*, 7th ed., Rosen, C.J. (Ed.), pp. 22–27. Washington, D.C.: American Society for Bone and Mineral Research.

Bonewald, L.F. & Johnson, M.L. (2008). Osteocytes, mechanosensing and Wnt signaling. *Bone* **42**, 606–615.

Bosetti, M. & Cannas, M. (2005). The effect of bioactive glasses on bone marrow stromal cells differentiation. *Biomaterials* **26**, 3873–3879.

Curtis, T.A., Ashrafi, S.H. & Weber, D.F. (1985). Canalicular communication in the cortices of human long bones. *Anat Rec* **212**, 336–344.

Feng, J.Q., Ward, L.M., Liu, S., Lu, Y., Xie, Y., Yuan, B., Yu, X., Rauch, F., Davis, S.I., Zhang, S., Rios, H., Drezner, M.K., Quarles, L.D., Bonewald, L.F. & White, K.E. (2006). Loss of DMP1 causes rickets and osteomalacia and identifies a role for osteocytes in mineral metabolism. *Nat Genet* **38**, 1310–1315.

Franz-Odendaal, T.A., Hall, B.K. & Witten, P.E. (2006). Buried alive: How osteoblasts become osteocytes. *Dev Dyn* **235**, 176–190.

Fukumoto, S. & Martin, T.J. (2009). Bone as an endocrine organ. *Trends Endocrinol Metab* **20**, 230–236.

Gorustovich, A., Porto López, J.M., Guglielmotti, M.B. & Cabrini, R.L. (2006). Biological performance of boron-modified bioactive glass particles implanted in rat tibia bone marrow. *Biomed Mater* **1**, 100–105.

Gorustovich, A., Rosenbusch, M. & Guglielmotti, M.B. (2002). Characterization of bone around titanium implants and bioactive glass particles: An experimental study in rats. *Int J Oral Maxillofac Implants* **17**, 644–650.

Gorustovich, A., Sivak, M.G. & Guglielmotti, M.B. (2007). A novel methodology for imaging new bone formation around bioceramic bone substitutes. *J Biomed Mater Res A* **8**, 443–445.

Gorustovich, A., Steimetz, T., Cabrini, R.L. & Porto López, J.M. (2010). Osteoconductivity of strontium-doped bioactive glass particles. A histomorphometric study in rats. *J Biomed Mater Res A* **92**, 232–237.

Hench, L.L. (1991). Bioceramics: From concept to clinic. *J Am Ceram Soc* **74**, 1487–1510.

Hench, L.L., Xynos, I.D. & Polak, J.M. (2004). Bioactive glasses for *in situ* tissue regeneration. *J Biomater Sci Polym* **15**, 543–562.

Kamioka, H., Honjo, T. & Takano-Yamamoto, T. (2001). A three-dimensional distribution of osteocyte processes revealed by the combination of confocal laser scanning microscopy and differential interference contrast microscopy. *Bone* **28**, 145–149.

Kamioka, H., Murshid, S.A., Ishihara, Y., Kajimura, N., Hasegawa, T., Ando, R., Sugawara, Y., Yamashiro, T., Takaoka, A. & Takano-Yamamoto, T. (2009). A method for observing silver-stained osteocytes *in situ* in 3-μm sections using ultrahigh voltage electron microscopy tomography. *Microsc Microanal* **15**, 377–383.

Knothe-Tate, M.L., Adamson, J.R., Tami, A.E. & Bauer, T.W. (2004). The osteocyte. *Int J Biomed Cell Biol* **36**, 1–8.

Knothe-Tate, M.L., Niederer, P. & Knothe, U. (1998). *In vivo* tracer transport through the lacunocanalicular system of rat bone in an environment devoid of mechanical loading. *Bone* **22**, 107–117.

Kokubo, T. & Takadama, H. (2006). How useful is SBF in predicting *in vivo* bone bioactivity? *Biomaterials* **27**, 2907–2915.

Lee, K.Y., Kim, H.M., Lim, Y.J., Chun, H.J., Kim, H. & Moon, S.H. (2006). Ceramic bioactivity: Progresses, challenges and perspectives. *Biomed Mater* **1**, 31–37.

Lu, Y., Xie, Y., Zhang, S., Dusevich, V., Bonewald, L.F. & Feng, J.Q. (2007). DMP1-targeted Cre expression in odontoblasts and osteocytes. *J Dent Res* **86**, 320–325.

Martin, D.M., Hallsworth, A.S. & Buckley, T. (1978). A method for the study of internal spaces in hard tissue matrices by SEM, with special reference to dentine. *J Microsc* **112**, 345–352.

Noble, B.S. (2008). The osteocyte lineage. *Arch Biochem Biophys* **473**, 106–111.

Okada, S., Yoshida, S., Ashrafi, S.H. & Schraufnagel, D.E. (2002). The canalicular structure of compact bone in the rat at different ages. *Microsc Microanal* **8**, 104–115.

Palumbo, C., Ferretti, M. & Marotti, G. (2004). Osteocyte dendrogenesis in static and dynamic bone formation: An ultrastructural study. *Anat Rec A Discov Mol Cell Evol Biol* **278**, 474–480.

Radin, S., Reilly, G., Bhargave, G., Leboy, P.S. & Ducheyne, P. (2005). Osteogenic effects of bioactive glass on bone marrow stromal cells. *J Biomed Mater Res* **73A**, 21–29.

Reilly, G.C., Knapp, H.F., Stemmer, A., Niederer, P. & Knothe-Tate, M.L. (2001). Investigation of the morphology of the lacunocanalicular system of cortical bone using atomic force microscopy. *Ann Biomed Eng* **29**, 1074–1081.

Schneider, P., Stauber, M., Voide, R., Stampanoni, M., Donahue, L.R. & Müller, R. (2007). Ultrastructural properties in cortical bone vary greatly in two inbred strains of mice as assessed by synchrotron light based micro- and nano-CT. *J Bone Miner Res* **22**, 1557–1570.

Sugawara, Y., Kamioka, H., Honjo, T., Tezuka, K. & Takano-Yamamoto, T. (2005). Three-dimensional reconstruction of chick calvarial osteocytes and their cell processes using confocal microscopy. *Bone* **36**, 877–883.

Teti, A. & Zallone, A. (2009). Do osteocytes contribute to bone mineral homeostasis? Osteocytic osteolysis revisited. *Bone* **44**, 11–16.

Weber, D.F. (1983). An improved technique for producing casts of the internal structure of hard tissues, including some observations on human dentine. *Arch Oral Biol* **28**, 885–891.

Xie, Y., Ye, L., Zhang, S., Dusevich, V. & Feng, J.Q. (2008). Visualization of osteocytes and mineralization. In *A Practical Manual for Musculoskeletal Research*, Leung, K.S., Qin, Y.X., Cheung, W.H. & Qin, L. (Eds.), pp. 135–145. Singapore: World Scientific Publishing Co.